Supporting Information

For

Nontargeted Screening of Aryl Hydrocarbon Receptor Agonists in Endangered Beluga Whales from the St. Lawrence Estuary: Beyond Legacy Contaminants

Holly Barrett[a], Jianxian Sun[a], Yuhao Chen[d], Diwen Yang[a], Jonathan Verreault[b], Magali Houde[c], Frank Wania[d], Hui Peng[*a,e]

[a] Department of Chemistry, University of Toronto, Toronto, ON M5S 3H6, Canada
[b] Centre de recherche en toxicologie de l'environnement (TOXEN), Département des sciences biologiques, Université du Québec à Montréal, P.O. Box 8888, Succursale Centre-ville, Montreal, QC H3C 3P8, Canada
[c] Environment and Climate Change Canada, 105 McGill Street, Montreal, QC H2Y 2E7, Canada
[d] Department of Physical and Environmental Sciences, University of Toronto Scarborough, 1265 Military Trail, Toronto, Ontario M1C 1A4, Canada
[e] School of the Environment, University of Toronto, Toronto, ON, Canada

***Corresponding author: Hui Peng**, e-mail: hui.peng@utoronto.ca, Department of Chemistry, University of Toronto, Toronto, Ontario, M5S3H6, Canada.

Text

S1. Sample Extraction. The ~10 g pooled tissue samples were homogenized in 50 mL falcon tubes using sterilized stainless steel dissection scissors. The samples were extracted based on an adapted version of the method previously used by Desforges *et al.*[1] Homogenized tissues were transferred to a 250 mL round-bottom flask. Tissues were extracted by sonication in 70 mL of acetone:hexane (5:2, v:v) for 30 min. To remove traces of water, extracts were filtered through a glass filter funnel finely packed with glass wool and pre-baked sodium sulfate into a separate pre-weighed 250 mL round-bottom flask. The acetone:hexane extraction was repeated a second time and the filtered extracts were combined and evaporated to dryness using a rotary evaporator. The flask was weighed to gravimetrically determine the total lipid content of the sample. Following this, 50 mL of acetonitrile was added to the lipid layer in the flask and vortexed to create a pseudo-

emulsion. The flask was placed in a −20 °C freezer for 1 hr to allow the lipids to solidify, and the acetonitrile layer was decanted into a clean round-bottom flask. A second 50 mL aliquot of acetonitrile was added to the lipid residue and the freeze-out step was repeated. The combined extracts were then evaporated to dryness using a rotary evaporator, reconstituted in 1 mL of acetonitrile, transferred to a 2 mL glass vial, and stored in a −20 °C freezer until further clean-up using gel permeation chromatography.

In order to remove any remaining trace amounts of lipids from the extracts, further clean-up was performed using gel permeation chromatography (GPC). Approximately 70 g of Bio-beads (S-X3 Beads, 200 – 400 Mesh; Bio-Rad, Canada), pre-soaked overnight in dichloromethane (DCM):hexane (50:50, v:v), were packed into a 250 mL reservoir glass PYREX® chromatography column (Fisher Scientific) which was pre-rinsed with acetone and hexane. 200 mL of DCM:hexane (50:50, v:v) was added to the column and was allowed to run through to waste until the solvent level was just below the surface of the beads. The 1 mL tissue extract was added to the surface of the beads using a glass Pasteur pipette, and the glass vial containing the extract was rinsed three times with 2 mL DCM:hexane (50:50, v:v) and transferred to the beads surface. The solvent was allowed to run through the column until the level was just below the beads surface. 75 mL of DCM:hexane (50:50, v:v) was added and allowed to run through the column until the level was just below the beads surface. This fraction contained the trace residual lipids from the extract and was discarded. Following this, a 200 mL aliquot of DCM:hexane (50:50, v:v) was added to the column and allowed to run through until the level was just below the beads surface, with the eluate being collected in a round-bottom flask. A 150 mL aliquot of DCM:hexane (50:50, v:v) was then added to the column to elute any remaining waste. This process was repeated for each of the four

pooled tissue extracts as well as a procedural blank, and the column was thoroughly rinsed with DCM:hexane (50:50, v:v) in between samples to minimize potential carry-over. Lastly, the tissue eluates were evaporated to dryness using a rotary evaporator and were reconstituted in 1 mL acetonitrile (final extract concentration ~ 10 g_{tissue}/mL). Extracts were stored in a −20 °C freezer until chemical analysis or application in receptor bioassays.

S2. AhR and MTT Bioassays.

In brief, H4IIE-luc cells were maintained in Dulbecco's Modified Eagle's Medium (DMEM; Sigma #D2902) without phenol red, supplemented with 10 % fetal bovine serum, 1 mM sodium pyruvate, 1 mg/mL bovine insulin, and 1 % penicillin-streptomycin at 37°C, 5 % CO_2, and 100 % humidity. The H4IIE-luc cells were plated in triplicate wells at a density of approximately 2 x 10^4 cells/well in 96-well plates and exposed after 24 h to a serial dilution of the reference chemical TCDD (62.5 – 1000 pM), solvent control (acetonitrile), or sample preparation control. Beluga tissue extracts were tested as a serial dilution of 5 concentrations (0.3 – 0.02 g/$mL_{extract}$) in triplicate wells. The concentration of solvent in test exposure media did not exceed 0.5 %. Exposures were conducted for 72 h under the same conditions as those used for culturing. In brief, 10 µL of MTT was incubated in each dose group for an additional 4 h after the cells were exposed to the beluga extracts. The MTT crystals formed after incubation were dissolved into dimethyl sulfoxide (DMSO) and absorbance was measured at 570 nm using a microplate reader (Tecan). For AhR activity measurements, after 72 h of exposure, the exposure media was removed, and the cells were washed twice with 75 µL of phosphate-buffered saline. Steadylite substrate mix (PerkinElmer) was used to assess AhR-mediated luciferase activity. Cells were lysed with 75 µL of steadylite substrate mix and 75 µL phosphate-buffered saline containing Ca^{2+} and Mg^{2+}, and plates were kept

in the dark for 20 min to allow complete lysis and enzymatic reaction. For luciferase activity measurement, a white sticker was placed at the bottom of the 96-well plate, and luminescence was measured with a microplate luminometer (Tecan).

S3. Chemical and Biological Potency Determination.

For AhR activity, sample responses from the H4IIE-luc bioassay were converted to percentages of the maximum response (% $TCDD_{max}$) observed for 1 nM TCDD (= 100 % $TCDD_{max}$).[2] The concentrations of TCDD-equivalent bioactivity (TCDD-EQ_{bio}) of beluga tissue extracts towards AhR potencies were obtained from dose-response relationships based on effective concentrations (ECs) at the 10 % level (EC_{10}) of samples with % $TCDD_{max}$ values of 10 % or greater.

The relative potency (ReP) of bromoindole toward AhR potency relative to TCDD was estimated on the basis of its 10 % of TCDD maximum induction (EC_{10}) value, obtained from the experimental dose-response curve of a 5-bromoindole chemical standard, using eq. 1.

$$ReP_{Bromoindole} = \frac{EC_{10(TCDD)}}{EC_{10(5-bromoindole)}} \qquad (1)$$

Then, the TCDD chemical equivalence (TCDD-EQ_{chem}) of AhR agonists in the beluga tissue extracts toward AhR potency was determined on the basis of their relative potencies in each extract, as per eq. 2.

$$TCDD - EQ_{chem} = \sum([AhR\ agonist]_i \times ReP_i) \qquad (2)$$

S4. LC-APCI-Orbitrap Analysis. One µL of each extract was applied to a C18 column (HALO, 2.7 µm, 2.1 x 100 mm; Canadian Life Science) and analyzed by a Vanquish ultrahigh-performance liquid chromatography (UHPLC) system (Thermo Fisher Scientific) coupled to a Q Exactive high-resolution mass spectrometer (Thermo Fisher Scientific). The sampler and column compartments

were maintained at 4 and 40 °C, respectively. The flow rate was 0.3 mL/min. The mobile phases were water (A) and acetonitrile (B). The LC method was as follows: B was increased from 20 % to 80 % from 0 to 3 min, increased to 100 % from 3 to 8 min, kept static from 8 to 12.5 min, and then returned to 20 % at 13 min and maintained at 20 % for 2 min.

Data were acquired in full scan and data-independent acquisition (DIA) mode, in both APCI (-) and APCI (+). Parameters for DIA were one full MS1 scan (100 − 1000 m/z) recorded at resolution R = 70 000 (at *m/z* 200) with a maximum of 3 × 106 ions collected within 100 ms, followed by seven DIA MS/MS scans recorded at a resolution R = 35 000 (at *m/z* 200) with a maximum of 1×10^5 ions collected within 50 ms. DIA data were collected by use of 10-*m/z*-wide isolation windows per MS/MS scan. Due to limited scanning speeds, eight different methods were run for each sample, and each method covered 200 Da mass ranges for DIA scanning (*i.e.*, 100 − 300 *m/z* for Method 1, 300 − 500 *m/z* for Method 2, and 500 − 700 *m/z* for Method 3, and 700 − 900 *m/z* for Method 4, for each of the + and – modes). The mass spectrometric settings used for APCI (−) mode were as follows: discharge current, 10 μA; sheath gas flow rate, 20 L/h; auxiliary gas flow rate, 5 L/h; probe heater temperature, 350 °C. The mass spectrometric settings used for APCI (+) mode were as follows: discharge current, 5 μA; sheath gas flow rate, 20 L/h; auxiliary gas flow rate, 5 L/h; probe heater temperature, 350 °C.

S5. LC-ESI-Orbitrap Analysis. LC-ESI-Orbitrap was used for suspect screening Tox21 compounds which are polar and ionizable under ESI. One μL of each extract was applied to a C18 column (HALO, 2.7 μm, 2.1 x 100 mm; Canadian Life Science) and analyzed by a Vanquish ultrahigh-performance liquid chromatography (UHPLC) system (Thermo Fisher Scientific) coupled to a Q Exactive high-resolution mass spectrometer (Thermo Fisher Scientific). The

sampler and column compartments were maintained at 4 and 40 °C, respectively. The flow rate was 0.3 mL/min. The mobile phases were ultrapure water (A) and methanol (B). The LC method was as follows: B was increased from 10 % to 100 % from 0 to 7 min, kept static from 7 to 11.5 min, and then returned to 10 % at 13 min and maintained at 10 % for 2 min.

Data were acquired in data-independent acquisition (DIA) mode in both ESI(-) and ESI(+) as described in a previous study.[3] Parameters for DIA were one full MS1 scan (100 − 1000 *m/z*) recorded at resolution R = 70 000 (at *m/z* 200) with a maximum of 3 × 106 ions collected within 100 ms, followed by seven DIA MS/MS scans recorded at a resolution R = 35 000 (at *m/z* 200) with a maximum of 1 × 105 ions collected within 50 ms. DIA data were collected by use of 10-*m/z*-wide isolation windows per MS/MS scan. Due to limited scanning speeds, eight different methods were run for each sample, and each method covered 200 Da mass ranges for DIA scanning (*i.e.*, 100 − 300 *m/z* for Method 1, 300 − 500 *m/z* for Method 2, and 500 − 700 *m/z* for Method 3, and 700-900 *m/z* for Method 4, for each of the + and – modes). The mass spectrometric settings used for ESI (−) mode were as follows: spray voltage, 2.7 kV; sheath gas flow rate, 30 L/h; auxiliary gas flow rate, 6 L/h; auxiliary gas heater temperature 300 °C, and capillary temperature 300 °C. The mass spectrometric settings used for ESI (+) mode were as follows: spray voltage, 3.00 kV; sheath gas flow rate, 40 L/h; auxiliary gas flow rate, 10 L/h; auxiliary gas heater temperature 350 °C, and capillary temperature 300 °C.

S6. Nontargeted Analysis of Halogenated Compounds.

The raw mass spectrometry files were converted to mzXML format, and the peaks were detected with the XCMS[4] package at a mass tolerance of 2.5 ppm. The peak features were matched across samples with a mass tolerance of 2.5 ppm and retention time window of 20 s after retention time

adjustment. Only peak features detected in beluga extracts at 10-fold higher intensities than in procedural blanks were kept for subsequent data analysis. Isotopic peaks of each peak feature were extracted and grouped according to their chromatographic co-elution profiles and exact *m/z*. An isotopic peak pattern filtering algorithm was used to select putative halogenated compounds. We focused particularly on chlorinated and brominated compounds for several reasons: 1) Fluorinated compounds were extensively investigated in our previous study[5]; 2) Iodinated compounds are rarely manufactured compared to brominated and chlorinated compounds;[6] 3) Brominated and chlorinated compounds have characteristic isotopic peak patterns that are detectable by nontargeted analysis.[7,8] Specifically, only the peak features with an isotopic peak (Δm= 1.9971 and 1.9980 for chlorinated and brominated compounds, respectively) at 25 % or greater intensity were selected. In-source fragments were further excluded via manual inspection if peak features were detected with the exact same retention time and chromatographic profiles. Formulas of detected peaks were predicted within a mass tolerance of 3 ppm, by constraining the number of chlorines and bromines based on isotopic peak patterns. Chemical formulas were set to contain up to 100 C, 200 H, 5 N, 30 O, 5 I, 10 Br, 10 Cl, and 2 S per molecule.

S7. Creation of a Tox21 *in silico* MS^2 Database.

The open-source machine learning MS^2 fragment prediction software, Competitive Fragmentation Modeling for Metabolite Identification version 4.0 (CFM-ID 4.0)[9], was used to develop a database of the *in silico* MS^2 fragments of all Tox21 compounds. The Tox21 chemical library consisting of 8,599 chemicals and their corresponding information (*e.g.,* CAS number) was downloaded from the U.S. EPA CompTox chemical dashboard (https://comptox.epa.gov/dashboard). Canonical SMILES were retrieved for each compound from PubChem using the webchem R package, and

compounds incompatible with CFM-ID (*i.e.,* metal-containing, salts) were removed from the dataset. CFM-ID prediction was applied to the remaining compounds in both negative ($[M-H]^-$) and positive ($[M+H]^+$) ESI modes. The resulting Tox21 *in silico* MS^2 database consisted of 5,795 and 5,845 compounds predicted in negative and positive mode, respectively. The final *in silico* database, which contains the Tox21 compounds and their corresponding chemical information (*m/z*, monoisotopic mass, molecular formula, CASN, SMILES, and predicted MS^2 fragments in negative or positive mode) was then generated. The negative and positive databases are provided in Data S2 and Data S3, respectively.

S8. Sulfuric Acid Treatment of Tissue Extracts.

Activated silica gel was impregnated with sulfuric acid (H_2SO_4; 90% in water, v/v) to a ratio of 1:2, w/w. 1 g of impregnated gel was then transferred to a Pasteur pipette packed with glass wool and 0.1 g of activated silica gel (0.1 g) at the bottom. 20 µL of beluga tissue extract (original concentration 10 g_{tissue}/mL) was transferred to an Eppendorf tube, evaporated to dryness under $N_{2(g)}$, and then reconstituted in 500 µL of DCM:hexane (50:50, v/v). The Pasteur pipette column was wetted with hexane prior to the addition of the 500 µL of extract. The sample was eluted with 5 mL 50:50 DCM:hexane, and the fraction was collected and blown to dryness under $N_{2(g)}$, and finally was reconstituted in 50 µL acetonitrile.

S9. GC-MS Analysis of PAHs.

Quantification of polycyclic aromatic hydrocarbons (PAHs) was achieved via an Agilent 7890 gas chromatograph (GC) coupled to a 7000 triple quadrupole tandem mass spectrometer operated in electron ionization mode. One µL of each extract was injected in pulsed splitless mode to a DB-5 column (J&W Scientific; 30 m, 0.250 mm diameter, 0.25 µm film thickness) with helium as the

carrier gas (flow rate = 2.25 $mL \cdot min^{-1}$). The detailed GC parameters (*e.g.,* temperatures, hold times) and the quantitative transitions used are provided in the SI (Table S4).

S10. PAHs were Not Major AhR Agonists in Beluga Tissues

Many PAHs are known AhR agonists,[10] and PAHs have previously been reported as contributors towards the AhR-mediated potencies of tissues of cetaceans including long-beaked common dolphins (*Delphinus capensis*) and fin whales (*Balaenoptera physalus*).[11] This inspired us to investigate the presence of PAHs in the beluga tissue extracts. Targeted analysis of 16 PAHs (see details in Text S9, Table S4) revealed the highest overall burden of PAHs was in the 2014 arctic blubber ($\sum_9$PAHs = 13.0 ng/$g_{tissue\ ww}$), followed by 2000s SLE liver ($\sum_9$PAHs = 8.69 ng/$g_{tissue\ ww}$), 1990s SLE blubber ($\sum_7$PAHs = 4.63 ng/$g_{tissue\ ww}$), and 2000s SLE blubber ($\sum_6$PAHs = 1.62 ng/$g_{tissue\ ww}$) (Figure S3). The higher concentration of ∑PAHs in 2000s SLE liver than 2000s SLE blubber was consistent with previous studies concerning the liver ($\sum_{14}$PAHs = 100 ng/g_{ww}) and blubber ($\sum_{13}$PAHs = 56 ng/g_{ww}) of a fin whale (*Balaenoptera physalus*) from Korea,[11] as well as the liver ($\sum_{14}$PAHs = 796.16 – 891.84 ng/g_{ww}) and blubber ($\sum_{13}$PAHs = 136.47 – 551.46 ng/g_{ww}) of sperm whales (*Physeter macrocephalus*) from Italy[12,13] and China[14]. While high trophic level marine mammals such as belugas are expected to rapidly metabolize PAHs, the higher accumulation of PAHs in SLE beluga liver may be related to recent PAHs exposure or the saturation of PAH-metabolizing enzymes in the whales.[15] Additionally, the concentration of ∑PAHs detected in the 2014 arctic blubber extract was comparable to that of a previous study involving the same specimen (∑PAHs concentration = ~5 ng/g_{lipid}).[16]

The lower concentrations of PAHs In SLE belugas were inconsistent with its higher activity, suggesting PAHs might not be major AhR agonists. To confirm this, we calculated the TCDD-EQ potency of the PAHs detected in the beluga tissues using their established ReP values (Figure

S4). ReP values for individual PAHs, based on the 25 % TCDD maximum induction (EC_{25}) for each PAH derived from a 72 h exposure of H4IIE-luc cells and the maximum response levels for the PAHs relative to TCDD, were obtained from the literature.[10] The calculated TCDD-EQ_{chem} for PAHs explained <1 % of the TCDD-EQ_{bio} of all four tissue extracts in the bioassay (Table S5. Collectively, while previous studies suggested that PAHs might be major AhR agonists using indirect evidence, our results demonstrated that PAHs are unlikely to be the major AhR agonists in both SLE belugas.

S11. Molecular Docking.

The binding affinity of compounds to AhR was modeled using the molecular docking software Autodock4 (v2.4.6; https://autodock.scripps.edu/) and its graphical front-end AutoDockTools. The three-dimensional structures of compounds (ligands) were obtained from PubChem in .sdf format and were converted to .pdb format via PyMOL 2.5 (v2.5.5; https://pymol.org/2/). Because the crystal structure of AhR has never been experimentally obtained from beluga whales, the predicted crystal structure of beluga AhR (bAhR; UniProt ID Q95LD9) was obtained from the AlphaFold Protein Structure Database in .pdb format (https://alphafold.ebi.ac.uk/). Twenty amino acid residues were assigned as contributing to the predicted bAhR ligand binding domain (LBD) cavity (PHE 286, THR 288, HIS 290, PHE 294, PRO 296, CYS 299, LEU 307, LEU 314, PHE 323, ILE 324, HIS 325, CYS 332, TYR 335, LEU 347, PHE 350, LEU 352, SER 364, ALA 366, ALA 380, and GLN 382) based on previous modeling of the bAhR TCDD binding fingerprint conducted by Pandini et al.[17] The model confidence for the bAhR LBD (residues 286 – 382) was reported by AlphaFold as ranging from 'High' to 'Very High', and therefore the predicted model was deemed suitable for LBD molecular docking analysis. The ligand and protein structures were then

converted to .pdbqt format via AutoDockTools. For the molecular docking, the grid box was set to encompass the region of the whole macromolecule consisting of the predicted LBD. The number of points in the x, y, and z dimensions were 50, 58, and 52, respectively. The parameters of the Genetic Algorithm (GA) of the docking were set as the default, except that the number of GA runs was increased to 50. For each docking, the lowest energy (ΔG) docked conformation out of all 50 runs, according to the Autodock scoring function, was selected for results visualization. The results of the docking (*e.g.,* hydrogen bonds, hydrophobic interactions) were visualized and imaged using PyMOL.

S12. Exposure-Activity Ratios (EARs).

EARs were calculated as follows:

$$EAR = \frac{Peak\ Intensity_{chemical}}{AC_{50}{}_{chemical}\ (\mu M)}$$

Wherein 'Peak Intensity$_{chemical}$' was the raw peak intensity of the chromatographic peak pertaining to the chemical obtained via LC-ESI-Orbitrap-MS, and '$AC_{50\ chemical}$' was the value of the half-maximal activity concentration, obtained from the Tox21 database, of the chemical towards AhR.

Table S1. Native and Mass-Labeled PCBs chemical standards used in the present study.

Compound Name	Abbreviation	*m/z* ([M-Cl+O]$^-$)
2-Chlorobiphenyl	PCB-1	169.0653
4-Chlorobiphenyl	PCB-3	169.0653
2,6-Dichlorobiphenyl	PCB-10	203.0264
4,4'-Dichlorobiphenyl	PCB-15	203.0264
2,2',6-Trichlorobiphenyl	PCB-19	236.9874
3,4,4'-Trichlorobiphenyl	PCB-37	236.9874
2,2',6,6'-Tetrachlorobiphenyl	PCB-54	270.9484
3,3',4,4'-Tetrachlorobiphenyl	PCB-77	270.9484
2,2',4,6,6'-Pentachlorobiphenyl	PCB-104	304.9095
3,3',4,4',5-Pentachlorobiphenyl	PCB-126	304.9095
2,2',4,4',6,6'-Hexachlorobiphenyl	PCB-155	338.8705
3,3',4,4',5,5'-Hexachlorobiphenyl	PCB-169	338.8705
2,2',3,4',5,6,6'-Heptachlorobiphenyl	PCB-188	372.8315
2,3,3',4,4',5,5'-Heptachlorobiphenyl	PCB-189	372.8315
2,2',3,3',4,4',6,6'-Octachlorobiphenyl	PCB-202	406.7925

2,3,3',4,4',5,5',6-Octachlorobiphenyl	PCB-205	406.7925
2,2',3,3',4,4',5,5',6-Nonachlorobiphenyl	PCB-206	440.7536
2,2',3,3',4,5,5',6,6'-Nonachlorobiphenyl	PCB-208	440.7536
Decachlorobiphenyl	PCB-209	474.7146
2,4,4'-Trichloro($^{13}C_{12}$)biphenyl	28L	249.0277
2,2',5,5'-Tetrachloro($^{13}C_{12}$)biphenyl	52L	282.9887
2,2',4,5,5'-Pentachloro($^{13}C_{12}$)biphenyl	101L	316.9497
2,2',3,4,4',5'-Hexachloro($^{13}C_{12}$)biphenyl	138L	350.9107
2,2',4,4',5,5'-Hexachloro($^{13}C_{12}$)biphenyl	153L	350.9107
2,2',3,4,4',5,5'-Heptachloro($^{13}C_{12}$)biphenyl	180L	384.8718
Decachloro($^{13}C_{12}$)biphenyl	209L	486.7549

Table S2. Recoveries of seven OH-BDEs using the sample extraction and cleanup procedure.

Compound Name	Chemical Formula	*m/z* ([M-H]$^-$)	Recovery (%)
3-OH-BDE7	$C_{12}H_8Br_2O_2$	340.8813	72 ± 5
6-OH-BDE-17	$C_{12}H_7Br_3O2$	418.7918	101 ± 15
6-OH-BDE-47	$C_{12}H_6Br_4O_2$	496.7023	117 ± 18
2-OH-BDE-123	$C_{12}H_5Br_5O_2$	574.6128	106 ± 12
6-OH-BDE-137	$C_{12}H_4Br_6O_2$	652.5233	75 ± 6
6-OH-Cl-BDE-17	$C_{12}H_6Br_3ClO_2$	452.7528	78 ± 9
6-OH-Cl-BDE-68	$C_{12}H_5Br_4ClO_2$	530.6633	91 ± 9

Table S3. Details of the three pooled SLE beluga whale tissue samples.

Sample Code	Sampling Year	Sex	Estimated Age	Age Group	Mass (g)
2000s SLE Liver					*11.1744*
DL2000-05	2000	F	50	Adult	1.0636
DL2001-01	2001	M	48	Adult	0.8875
DL2002-07	2002	M	45	Adult	0.9503
DL2003-02	2003	F	45	Adult	0.4342
DL2004-01	2004	F	12	Adult	0.5501
DL2005-01	2005	M	38	Adult	0.3940
DL2006-02	2006	F	4	Juvenile	0.6980
DL2007-09	2007	M	50	Adult	0.5103
DL2009-05	2009	F	48	Adult	0.8408
DL2010-08	2010	F	31	Adult	0.8543
DL2011-08	2011	F	22	Adult	0.8637
DL2013-03	2013	M	41	Adult	0.8517
DL2015-04	2015	F	33	Adult	0.7322
DL2016-01	2016	F	15	Adult	0.5612
DL2017-01	2017	F	53	Adult	0.9825
2000s SLE Blubber					*9.9972*
DL2000-01	2001	M	48	Adult	1.2065
DL2002-08	2002	M	28	Adult	0.6957
DL2003-02	2003	F	45	Adult	1.1017
DL2004-04	2004	M	3	Juvenile	1.3125
DL2005-01	2005	M	38	Adult	1.4520
DL2006-01	2006	M	55	Adult	0.2150
DL2007-03	2007	F	50	Adult	0.6816
DL2009-02	2009	M	1	Juvenile	0.6037
DL2012-02	2012	M	23	Adult	0.8848
DL2013-07	2013	M	54	Adult	0.7402
DL2015-06	2015	F	33	Adult	0.8615
DL2017-01	2017	F	53	Adult	0.2420
1990s SLE Blubber					*9.2676*
DL1993-07	1993	F	29	Adult	2.0026
DL1993-08	1993	F	16	Adult	1.3757
DL1995-12	1995	M	19	Adult	1.6170
DL1995-07	1995	M	1	Juvenile	0.9597
DL1996-09	1996	M	50	Adult	1.2373
DL1996-01	1996	M	42	Adult	1.5162
DL1998-07	1998	M	36	Adult	0.5591

Table S4. GC-MS/MS method parameters for the analysis of PAHs.

Analyte	Retention Time (min)	Quantitative			Qualitative		
		Precursor Ion	Product Ion	CE (eV)	Precursor Ion	Product Ion	CE (eV)
Naphthalene	5.38	128.0	102.0	22	128.0	127.0	22
Acenaphthylene	8.80	152.0	150.0	40	152.0	151.0	40
Acenaphthene	9.24	154.0	152.0	40	153.0	152.0	40
Fluorene	10.42	166.0	165.0	30	165.0	163.0	34
Anthracene	12.67	178.0	152.0	20	178.0	176.0	34
Phenanthrene	12.77	178.0	152.0	20	178.0	176.0	34
Pyrene	15.51	202.0	201.0	30	202.0	200.0	50
Fluoranthene	16.02	202.0	201.0	30	202.0	200.0	50
Chrysene	19.23	228.0	226.0	38	228.0	224.0	38
Benzo(b)fluoranthene	22.44	252.0	250.0	42	250.0	248.0	40
Benzo(k)fluoranthene	22.51	252.0	250.0	42	250.0	248.0	40
Benzo(α)pyrene	23.36	252.0	250.0	42	250.0	248.0	40
Indeno(1,2,3-cd)pyrene	26.86	276.0	274.0	42	277.0	275.0	42
Dibenzo(a,b)anthracene	26.97	278.0	276.0	38	277.0	274.0	40
Benzo(g,h,i)perylene	27.62	276.0	274.0	30	277.0	275.0	40
D_8 – Naphthalene	5.35	136.1	108.2	22			
D_8 – Acenaphthylene	8.79	160.0	158.0	40			
D_{10} – Fluorene	10.38	176.0	174.0	30			
D_{10} – Phenanthrene	12.64	188.0	160.0	34			
D_{10} – Pyrene	15.49	212.0	210.0	30			
D_{10} – Fluoranthene	16.01	212.0	210.0	30			
D_{12} – Chrysene	19.20	240.0	236.0	38			
D_{12} – Benzo(α)pyrene	23.37	264.0	260.3	42			
D_{12} – Benzo(g,h,i)perylene	27.60	288.0	284.0	38			

Instrument Parameter	Setting
Inlet temperature	280 °C
GC-MS/MS Interface Temperature	310 °C
Ion Source Temperature	230 °C
MS1 Quadrupole Temperature	150 °C
MS2 Quadrupole Temperature	150 °C
Initial Temperature (Hold Time)	90 °C (1 minute)
Temperature Increase 1	10 °C/minute to 250 °C
Temperature Increase 2	5 °C/minute to 300 °C
Final Temperature (Hold Time)	300 °C (4 minutes)

Table S5. Summary of Tox21 screening hits (CL = 1-3) detected in beluga tissue extracts (2000s SLE liver, 2000s SLE blubber, and 2014 Arctic blubber).

m/z	Compound	CASRN	CL
226.1337	o-Aminoazotoluene	97-56-3	1
399.3469	Diisononyl adipate	33703-08-1	1
296.1162	Triadimenol	55219-65-3	1
218.1538	Ethoxyquin	91-53-2	1
153.0545	4-Hydroxy-3-methoxybenzaldehyde	121-33-5	1
280.1536	Metalaxyl	57837-19-1	1
325.1911	Quinidine	56-54-2	2a
165.1386	N,N,N',N'-Tetramethyl-p-phenylenediamine	100-22-1	2a
153.0545	Methylparaben	99-76-3	2a
222.1234	Formetanate hydrochloride	23422-53-9	2a
288.1591	Galanthamine	357-70-0	2b
229.1223	Nabumetone	42924-53-8	2b
255.1850	4,4'-Methylenebis(N,N-dimethylaniline)	101-61-1	2b
153.1273	3,7-Dimethyl-2,6-octadienal	5392-40-5	2b
176.0703	Indole-3-acetic acid	87-51-4	2b
159.0916	1,5-Naphthalenediamine	2243-62-1	2b
199.1228	4,4'-Diaminobiphenyl methane	101-77-9	2b
175.0864	1-Phenyl-3-methyl-5-pyrazolone	89-25-8	2b
175.0965	Diethyl butanedioate	123-25-1	2b
285.2073	2,2,4-Trimethyl-1,3-pentanediol diisobutyrate	6846-50-0	2b
219.1388	alpha,alpha-Dimethylphenethyl butyrate	10094-34-5	2b
235.1338	Heptyl p-hydroxybenzoate	1085-12-7	2b
235.2054	Isocyclemone E	54464-57-2	2b
287.2372	Retinol	68-26-8	2b
213.1634	2,6-Diisopropylnaphthalene	24157-81-1	2b
239.0712	Chrysarobin	491-59-8	3
317.2476	Methyl abietate	127-25-3	3
228.1028	Methfuroxam	28730-17-8	3
281.1103	Fanetizole	79069-94-6	3
191.0702	Piperonal acetone	3160-37-0	3
207.1022	Pentylparaben	6521-29-5	3
277.1543	Pifoxime	31224-92-7	3
194.1539	4-Hexyloxyaniline	39905-57-2	3
165.1386	N,N-Diethyl-p-phenylenediamine	93-05-0	3
221.0958	3-Acetylphenanthrene	2039-76-1	3
207.0813	2-Acetylfluorene	781-73-7	3
422.1756	Fluvastatin	93957-54-1	3
208.0968	N-(2-Methoxyphenyl)-3-oxobutanamide	92-15-9	3
237.1846	1-O-Hexyl-2,3,5-trimethylhydroquinone	148081-72-5	3
311.2014	Cannabinol	521-35-7	3
183.0653	Flopropione	2295-58-1	3
207.0694	2-Hydrazino-4-(4-aminophenyl) thiazole	26049-71-8	3
181.1221	Olivetol	500-66-3	3

Table S6. Potency balance between TCDD-EQ_{chem} and TCDD-EQ_{bio} concentrations in beluga tissue extracts (N.D. = not detected).

Compound	2000s SLE Liver	2000s SLE Blubber	2014 Arctic Blubber
TCDD-EQ_{chem} (ng/g_{ww})[a]			
Bromoindole	9.52E-04	N.D.	N.D.
Benzo(α)anthracene	1.11E-07	3.85E-08	5.85E-08
Chrysene	N.D.	1.51E-06	1.94E-06
ΣTCDD-EQ_{chem} (ng/g_{ww})	9.52E-04	1.55E-06	2.00E-06
TCDD-EQ_{bio} (ng/g_{ww})	8.29E-02	6.02E-02	4.78E-02
Contribution (%)	1.15	0.003	0.004

[a]Calculated by multiplying the concentrations of the AhR agonists by their ReP values.

Table S7: Top 10 highest EAR Tox21 hits (CL = 1 – 2b) across beluga tissue extracts (2000s SLE liver, 2000s SLE blubber, and 2014 Arctic blubber).

Compound	CL	Functional Use(s)[a]	SLE Liver		SLE Blubber (2000s)		Arctic Blubber (2014)	
			EAR	% Contribution[b]	EAR	% Contribution[b]	EAR	% Contribution[b]
o-Aminoazotoluene	1	Dyes	1.64E+05	46.5	N.D.	N.D.	N.D.	N.D.
Galanthamine	2b	Pharmaceutical	4.66E+04	13.2	N.D.	N.D.	N.D.	N.D.
Nabumetone	2b	Pharmaceutical	1.12E+03	0.3	4.43E+04	96.9	N.D.	N.D.
4,4'-Methylenebis(N,N-dimethylaniline)	2b	Dyes	4.16E+04	11.8	N.D.	N.D.	N.D.	N.D.
3,7-Dimethyl-2,6-octadienal		Fragrance, flavouring	3.77E+04	10.7	5.10E+02	1.1	1.54E+02	63.9
Indole-3-acetic acid	2b	Natural Product	2.41E+04	6.8	8.95E+02	2.0	8.69E+01	36.1
1,5-Naphthalenediamine	2b	Dyes, elastomers, pharmaceuticals	1.57E+04	4.5	N.D.	N.D.	N.D.	N.D.
Quinidine	2a	Pharmaceutical	8.05E+03	2.3	N.D.	N.D.	N.D.	N.D.
Diisononyl adipate	1	Cosmetics, lubricants, plasticizers	7.79E+03	2.2	N.D.	N.D.	N.D.	N.D.
4,4'-Diaminobiphenyl methane	2b	Dyes, adhesives, curing agents, cosmetics, rubber processing	6.25E+03	1.8	N.D.	N.D.	N.D.	N.D.

[a]From PubChem

[b]Represents the contribution (%) towards the ΣEAR of the top 10 highest Tox21 hits.

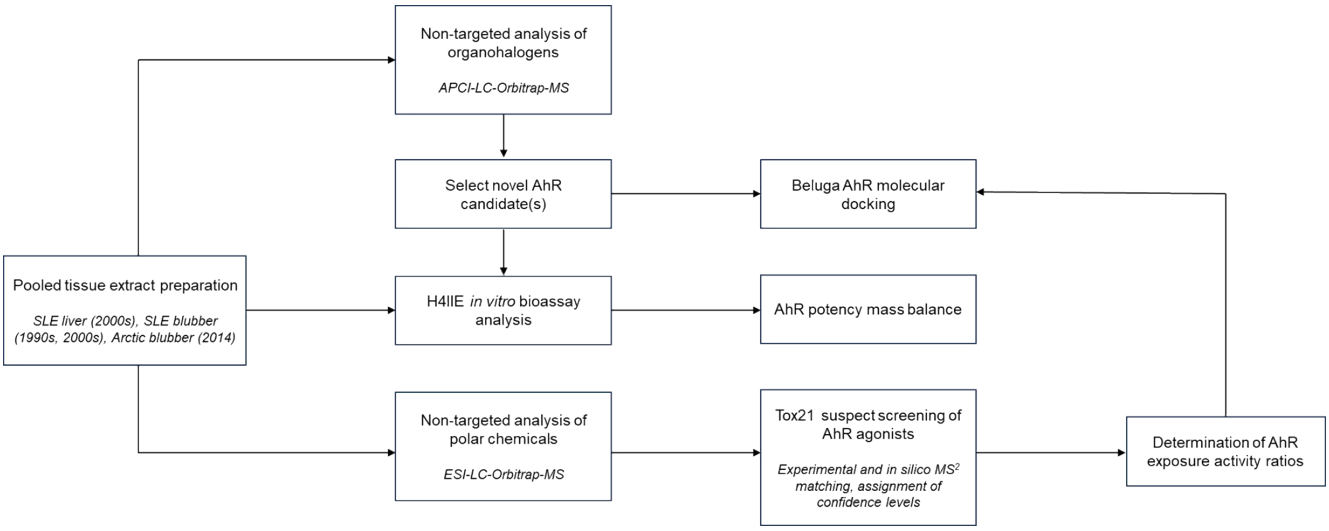

Figure S1. Workflow of the present study.

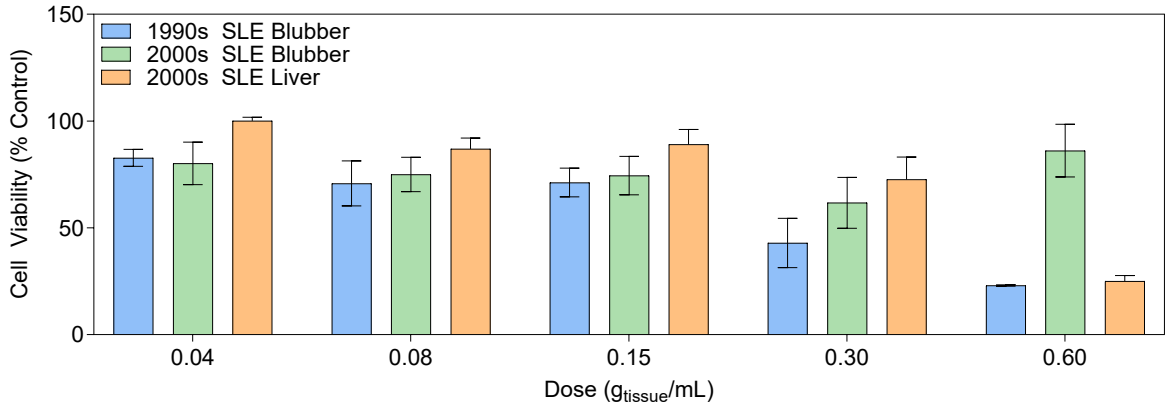

Figure S2. 1990s SLE blubber was found to be cytotoxic via MTT assay. Error bars represent the mean ± SD; n = 3.

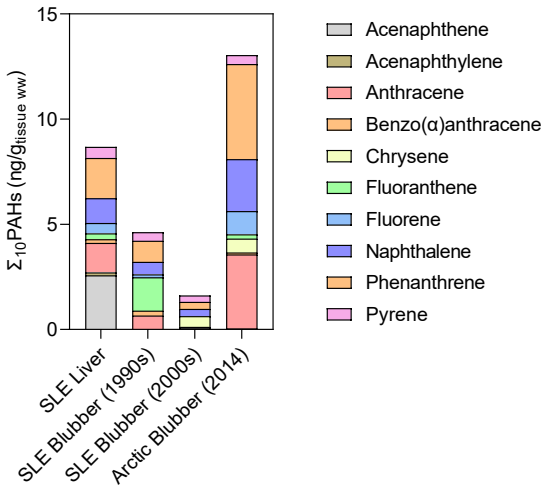

Figure S3. PAHs concentrations in beluga extracts obtained from GC-MS/MS analysis.

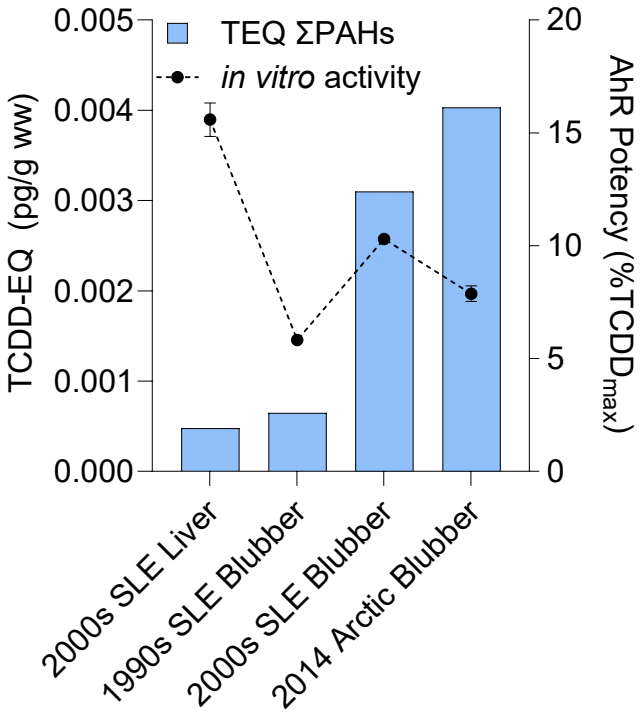

Figure S4. Calculated TEQ-∑PAHs was the highest for arctic blubber (shown alongside the in vitro AhR activity of the extracts at a dose of 300 g_{tissue}/L), indicating that the AhR potency of the arctic beluga can be partially explained by AhR-active PAHs. (Error bars represent the mean ± SD; n = 3)

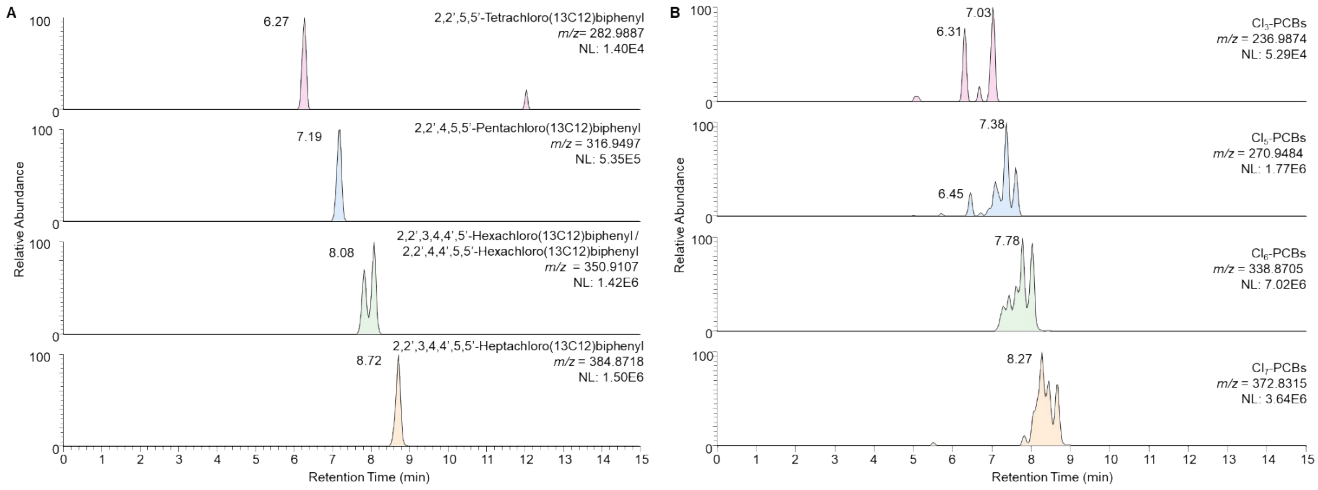

Figure S5. Validation of PCBs using mass-labeled chemical standards. (A) chemical standard (B) 2000s SLE blubber.

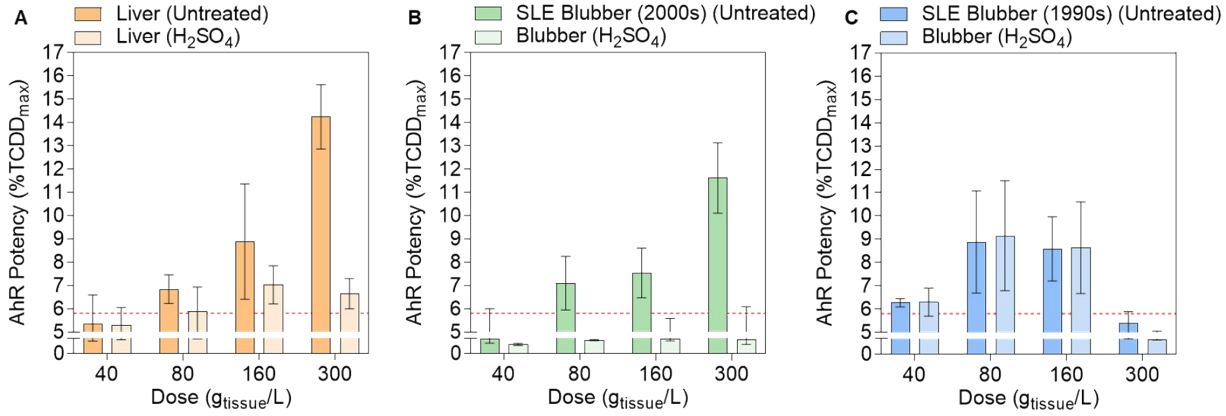

Figure S6. Sulfuric acid treatment of beluga extracts depleted the AhR potency of 2000s SLE liver and 2000s SLE blubber but not 1990s SLE blubber.

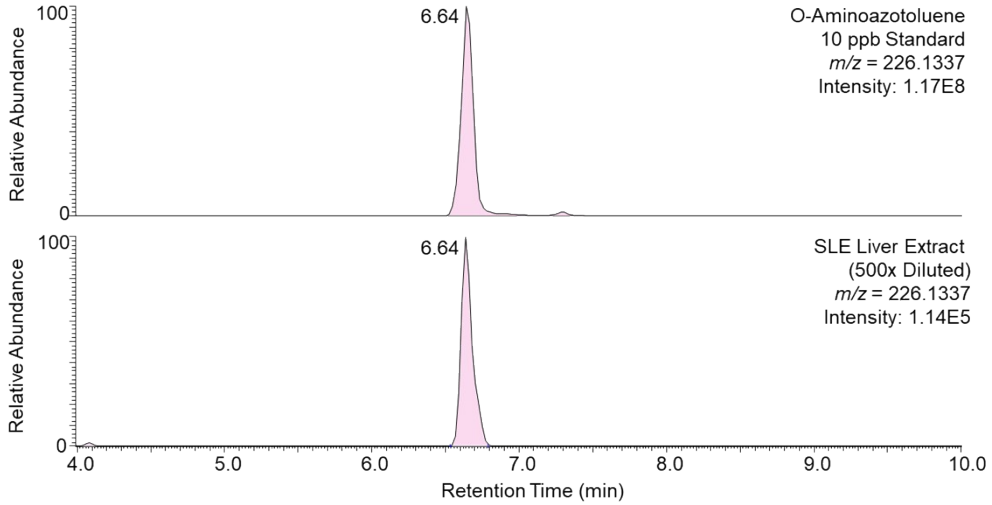

Figure S7. Confirmation of o-Aminoazotoluene in the 2000s SLE liver sample via chemical standard.

References

1 J. P. Desforges, I. Eulaers, L. Periard, C. Sonne, R. Dietz and R. J. Letcher, A rapid analytical method to quantify complex organohalogen contaminant mixtures in large samples of high lipid mammalian tissues, *Chemosphere*, 2017, **176**, 243–248.

2 J. Kim, S. Hong, J. Cha, J. Lee, T. Kim, S. Lee, H. B. Moon, K. H. Shin, J. Hur, J. S. Lee, J. P. Giesy and J. S. Khim, Newly Identified AhR-Active Compounds in the Sediments of an Industrial Area Using Effect-Directed Analysis, *Environ. Sci. Technol.*, 2019, **53**, 10043–10052.

3 H. Peng, C. Chen, D. M. V. Saunders, J. Sun, S. Tang, G. Codling, M. Hecker, S. Wiseman, P. D. Jones, A. Li, K. J. Rockne and J. P. Giesy, Untargeted Identification of Organo-Bromine Compounds in Lake Sediments by Ultrahigh-Resolution Mass Spectrometry with the Data-Independent Precursor Isolation and Characteristic Fragment Method, *Analytical Chemistry*, 2015, **87**, 10237–10246.

4 C. A. Smith, E. J. Want, G. O. Maille, R. Abagyan and G. Siuzdak, XCMS: Processing Mass Spectrometry Data for Metabolite Profiling Using Nonlinear Peak Alignment, Matching, and Identification, *Analytical Chemistry*, 2006, **78**, 779–787.

5 H. Barrett, X. Du, M. Houde, S. Lair, J. Verreault and H. Peng, Suspect and Nontarget Screening Revealed Class-Specific Temporal Trends (2000-2017) of Poly- And Perfluoroalkyl Substances in St. Lawrence Beluga Whales, *Environ. Sci. Technol.*, 2021, **55**, 1659–1671.

6 H. Peng, C. Chen, J. Cantin, D. M. V. Saunders, J. Sun, S. Tang, G. Codling, M. Hecker, S. Wiseman, P. D. Jones, A. Li, K. J. Rockne, N. C. Sturchio, M. Cai and J. P. Giesy, Untargeted Screening and Distribution of Organo-Iodine Compounds in Sediments from Lake Michigan and the Arctic Ocean, *Environ. Sci. Technol.*, 2016, **50**, 10097–10105.

7 H. Peng, C. Chen, D. M. V. Saunders, J. Sun, S. Tang, G. Codling, M. Hecker, S. Wiseman, P. D. Jones, A. Li, K. J. Rockne and J. P. Giesy, Untargeted Identification of Organo-Bromine

Compounds in Lake Sediments by Ultrahigh-Resolution Mass Spectrometry with the Data-Independent Precursor Isolation and Characteristic Fragment Method, *Anal. Chem.*, 2015, **87**, 10237–10246.
8 S. Kutarna, S. Tang, X. Hu and H. Peng, Enhanced Nontarget Screening Algorithm Reveals Highly Abundant Chlorinated Azo Dye Compounds in House Dust, *Environ. Sci. Technol.*, 2021, **55**, 4729–4739.
9 F. Wang, J. Liigand, S. Tian, D. Arndt, R. Greiner and D. S. Wishart, CFM-ID 4.0: More Accurate ESI-MS/MS Spectral Prediction and Compound Identification, *Anal. Chem.*, 2021, **93**, 11692–11700.
10 M. Larsson, D. Orbe and M. Engwall, Exposure time-dependent effects on the relative potencies and additivity of PAHs in the Ah receptor-based H4IIE-luc bioassay, *Environmental Toxicology and Chemistry*, 2012, **31**, 1149–1157.
11 J. Cha, S. Hong, J. Lee, J. Gwak, M. Kim, S. Mok, H.-B. Moon, P. D. Jones, J. P. Giesy and J. S. Khim, Identification of Mid-Polar and Polar AhR Agonists in Cetaceans from Korean Coastal Waters: Application of Effect-Directed Analysis with Full-Scan Screening, *Environmental Science*, 2023, **57**, 15644–15655.
12 L. Marsili, S. Maltese, D. Coppola, L. Carletti, S. Mazzariol and M. C. Fossi, Ecotoxicological status of seven sperm whales *(Physeter macrocephalus)* stranded along the Adriatic coast of Southern Italy, *Aquatic Conservation*, 2014, **24**, 103–118.
13 S. Mazzariol, G. Di Guardo, A. Petrella, L. Marsili, C. M. Fossi, C. Leonzio, N. Zizzo, S. Vizzini, S. Gaspari, G. Pavan, M. Podestà, F. Garibaldi, M. Ferrante, C. Copat, D. Traversa, F. Marcer, S. Airoldi, A. Frantzis, Y. De Bernaldo Quirós, B. Cozzi and A. Fernández, Sometimes Sperm Whales (Physeter macrocephalus) Cannot Find Their Way Back to the High Seas: A Multidisciplinary Study on a Mass Stranding, *PLoS ONE*, 2011, **6**, e19417.
14 F. Zhan, X. Yu, X. Zhang, L. Chen, X. Sun, R. Yu and Y. Wu, Tissue distribution of organic contaminants in stranded pregnant sperm whale (Physeter microcephalus) from the Huizhou coast of the South China Sea, *Marine Pollution Bulletin*, 2019, **144**, 181–188.
15 R. A. Lourenço, S. Taniguchi, J. Da Silva, F. D. C. Gallotta and M. C. Bícego, Polycyclic aromatic hydrocarbons in marine mammals: A review and synthesis, *Marine Pollution Bulletin*, 2021, **171**, 112699.
16 M. J. Binnington, Effects of preparation on nutrient and environmental contaminant levels in Arctic beluga whale (Delphinapterus leucas) traditional foods, *Environmental Science: Processes & Impacts*, 2017, **19**, 1000–1015.
17 A. Pandini, A. A. Soshilov, Y. Song, J. Zhao, L. Bonati and M. S. Denison, Detection of the TCDD Binding-Fingerprint within the Ah Receptor Ligand Binding Domain by Structurally Driven Mutagenesis and Functional Analysis, *Biochemistry*, 2009, **48**, 5972–5983.